Biochimica et Biophysica Acta 1793 (2009) 528–539

Contents lists available at ScienceDirect

Biochimica et Biophysica Acta

journal homepage: www.elsevier.com/locate/bbamcr

Lysophospholipids stimulate prostate cancer cell migration via TRPV2 channel activation

Michaël Monet [a,b], Dimitra Gkika [a,b], V'yacheslav Lehen'kyi [a,b], Albin Pourtier [c], Fabien Vanden Abeele [a,b], Gabriel Bidaux [a,b], Véronique Juvin [d], François Rassendren [d], Sandrine Humez [a,b,e], Natalia Prevarsakaya [a,b,*]

[a] Inserm, U-800, Equipe labellisée par la Ligue Nationale contre le cancer, Villeneuve d'Ascq, F-59655 France
[b] Université des Sciences et Technologies de Lille (USTL), Villeneuve d'Ascq, F-59655, France
[c] UMR 8161 Institut de Biologie de Lille CNRS/Université Université Lille 1 et 2/Institut Pasteur de Lille, 1 rue du Professeur Calmette, Lille, F-59000 France
[d] Département de Pharmacologie, Institut de Génomique Fonctionnelle, CNRS UMR 5203, INSERM U661, Université Montpellier I, Université Montpellier II, 141 rue de la Cardonille, Montpellier Cedex, F-34396 France
[e] Université d'Artois, Faculté des Sciences Jean Perrin, rue Jean Souvraz, Lens, F-62300 France

ARTICLE INFO

Article history:
Received 2 September 2008
Received in revised form 30 December 2008
Accepted 5 January 2009
Available online 15 January 2009

Keywords:
TRPV2
Lysophospholipid
Calcium
Translocation
Prostate cancer
Cell migration

ABSTRACT

The physiological role, the mechanisms of activation, as well as the endogenous regulators for the non-selective cationic channel TRPV2 are not known so far. In the present work we report that endogenous lysophospholipids such as lysophosphatidylcholine (LPC) and lysophosphatidylinositol (LPI) induce a calcium influx via TRPV2 channel. This activation is dependent on the length of the side-chain and the nature of the lysophospholipid head-group. TRPV2-mediated calcium uptake stimulated by LPC and LPI occurred via Gq/Go-protein and phosphatidylinositol-3,4 kinase (PI3,4K) signalling. We have shown that the mechanism of TRPV2 activation induced by LPC and LPI is due to the TRPV2 channel translocation to the plasma membrane. The activation of TRPV2 channel by LPC and LPI leads to an increase in the cell migration of the prostate cancer cell line PC3. We have demonstrated that TRPV2 is directly involved in both steady-state and lysophospholipid-stimulated cancer cell migration. Thus, for the first time, we have identified one of the natural regulators of TRPV2 channel, one of the mechanisms of TRPV2 activation and regulation, as well as its pathophysiological role in cancer.

1. Introduction

Calcium constitutes an essential intracellular messenger to a plethora of cell signal transduction pathways and a number of important physiological functions. In non-excitable cells, transient receptor potential (TRP) channels play an important role in cytosolic calcium regulation [1]. Given the importance of calcium signalling in all cell types, it is not surprising that dysfunctions in Ca^{2+}-permeable channels may eventually contribute to the pathogenesis of different diseases. The TRP family of channels is divided into seven related subfamilies: TRPC, TRPV, TRPM, TRPP, TRPN, TRPA and TRPML [2–4]. TRP channels have received considerable attention over the past decade and a number of remarkable properties and modes of regulation have been discovered for most of them, allowing us to understand such fundamental physiological functions as thermosensing, taste or calcium absorption [5]. However, TRPV2 (initially named VRL-1), a member of the TRP vanilloid, TRPV, channel subfamily, remains one of the most mysterious, since both its physiological and/or pathophysiological function, the mechanisms of its activation and the identity of the endogenous channel regulators are still unknown.

TRPV2 is expressed in sensory neurons and was initially detected in tissues having no role in thermosensation, such as the digestive tract and prostate [6,7]. Furthermore, in non-neuronal cells mechanisms other than temperature have been reported to activate TRPV2, such as the chemotactic peptide fMetLeuPhe [8] or growth factors inducing dynamic insertion into the plasma membrane [9], regulation by a phosphatidylinositol-3 kinase (PI3K) dependent pathway [10], or mechano- and osmotic stimuli [11,12]. In addition, despite the findings that 2-APB (2-aminoethoxydiphenyl borate) [13] and noxious heat (>52 °C) activate rat and mouse TRPV2 (*r*, mTRPV2), neither of these stimuli has been shown to activate human TRPV2 (hTRPV2) [14,15].

Several endogenous molecules have been shown to activate TRP channels including membrane phospholipids, such as phosphatidylinositol 4,5-bisphosphate (PIP2) or lysophospholipids (LPC and LPI). It has recently been shown that TRPC5 and TRPM8 could be activated by lysophospholipids [16,17], and a number of TRP channels (TRPV1, TRPV5, TRPM4, TRPM5, TRPM7, TRPM8) could be regulated by PIP_2 and fatty acid derivatives [18]. In an effort to further understand TRPV2 function and physiological activation, it was our aim to investigate TRPV2-

* Corresponding author. Laboratoire de Physiologie Cellulaire Inserm U-800, Bâtiment SN3, USTL, 59650 Villeneuve d'Ascq, France. Tel.: +33 3 20 33 64 23; fax: +33 3 20 43 40 66.
E-mail address: natacha.prevarskaya@univ-lille1.fr (N. Prevarsakaya).

0167-4889/$ – see front matter © 2009 Elsevier B.V. All rights reserved.
doi:10.1016/j.bbamcr.2009.01.003

mediated Ca^{2+} influxes in response to physiological lipids. We have identified some lysophospholipids as new physiological stimuli for TRPV2 channel. This mechanism is very important since it has been suggested that lysophospholipids have a range of physiological and pathological effects [19,20], including the stimulation of cancer cell migration [21,22]. The latter has also been a focus of our studies.

2. Experimental procedures

2.1. Chemicals and lipid preparation

LPCs, a mix of fatty acids (Lipid Standards: Fatty Acid Methyl Ester mixtures), LPI (L-α-lysophosphatidylinositol), LPE (3-*sn*-Lysophosphatidylethanolamine), LPA (Oleoyl-L-α-lysophosphatidic acid sodium salt) and S1P (Sphingosine 1-phosphate), were dissolved into methanol. The final bath solvent concentration was ≤0.1% and was present in the control period prior to application of the lipid molecule. No solvent effects were evident (*e.g.* see Figs. 1I and 2G). L-α-Lysophosphatidylcholine (soybean), L-α-caproyl lysophosphatidylcholine (LPC C6:0), L-α-lauroyl lysophosphatidylcholine (LPC C12:0), 3-*sn*-1-myristoyl-lysophosphatidylcholine (LPC C14:0), L-α-palmitoyl lysophosphatidylcholine (LPC C16:0), 1-Stearoyl-*sn*-glycero-3-phosphocholine (LPC C18:0), 1-Oleoyl-*sn*-glycero-3-phosphocholine (LPC C18:1), LPI (L-α-lysophosphatidylinositol soybean), LPE (3-*sn*-Lysophosphatidylethanolamine), LPA (Oleoyl-L-α-lysophosphatidic acid sodium salt), S1P (Sphingosine 1-phosphate), a mix of fatty acids (Lipid Standards: Fatty Acid Methyl Ester mixtures), choline (2-hydroxyethyl trimethylammonium hydroxide), arachidonic acid, pertussis toxin (PTX), wortmannin, and LY294002 were purchased from Sigma. If not mentioned otherwise, LPC (LPC CTL) corresponds to L-α-Lysophosphatidylcholine (soybean).

2.2. Cell culture

Human Embryonic Kidney 293 (HEK293) and Prostate Carcinoma 3 (PC3) cells were cultured as previously described [23,24]. Chinese Hamster Ovary K1 (CHO-K1) and stable CHO cell lines expressing mouse TRPV2 (clone IIE11) were cultured as previously described [15].

2.3. Generation of shTRPV2 vectors

Hybridized oligonucleotides were cloned in pSilencer 4.1-CMV puro (Ambion, Courtaboeuf, France) following the manufacturer's instructions and were defined as shTRPV2-1 (sense 5′-GGTAAGACGTGCCTGATGA-3′) and shTRPV2-2 (sense 5′ TAAGAGTCAACCTCAACTA-3′). Silencing efficiency was checked by western-blotting and PCR.

2.4. Nucleofection

Transfection of HEK293 or PC3 cells with hTRPV2-GFP or with shTRPV2-1 and -2 was carried out using Nucleofector, as recommended by the manufacturer (Amaxa GmbH, Köln, Germany). 3 μg of a vector were transfected into 2 million trypsinized cells, which were then seeded into a T75 flask and on glass slips for 72 h. For HEK293, cells were always co-nucleofected with a plasmid encoding two shRNAs TRPV2 (HEKhTRPV2-shV2 I or II) used to knockdown hTRPV2 channel expression or with pSilencer used as a negative control (HEKhTRPV2). Expression of hTRPV2-GFP channel was detected 72 h after nucleofection by GFP fluorescence using HEKhTRPV2 cells.

2.5. Reverse transcription-PCR

Total RNAs were isolated from PC3 cells followed by PCR as previously described [23]. Primers used are listed in Table 1. Then, density measurements were performed with "Quantity one" software (Biorad) and the data were analyzed using Origin 7.0 (Microcal Software Inc., Northampton, MA, USA).

2.6. Immunodetection

HEK293 and CHO cells were fixed with 4% formaldehyde-1X PBS (Phosphate Buffer Saline) for 15 min, washed three times, then permeabilized in PBS-gelatin 1.2% complemented with 0.01% Tween 20 and 100 mM glycine for 30 min at 37 °C. Subsequently, cells were incubated with primary antibodies: (1/250) rabbit polyclonal anti-hTRPV2 antibody for HEK293 and (1/250) rabbit polyclonal anti-mTRPV2 antibody for CHO cells, (1/25) in PBS-gelatin at 37 °C for 1.5 h. After thorough washes, the slides were treated with the corresponding anti-rabbit or anti-mouse IgG, coupled with Alexa fluor 488-labeleld (Molecular probes, dilution: 1/2000) diluted in PBS-gelatin for 1 h at room temperature. After two washes, the slides were mounted with Mowiol®. Fluorescence analysis was carried out using a Zeiss LSM 510 confocal microscope and analysis software (AIM 3.2, Zeiss), as previously described [23].

2.7. Ca^{2+} measurements using Fura-2 AM

Prior to fluorescence measurements, cells were trypsinized and transferred to glass slips. Cells were used 3 days after trypsinization. The medium was replaced every 48 h. The culture medium was replaced by an HBSS solution containing 142 mM NaCl, 5.6 mM KCl, 1 mM $MgCl_2$, 2 mM $CaCl_2$, 0.34 mM Na_2HPO_4, 0.44 mM KH_2PO_4, 10 mM HEPES, and 5.6 mM glucose. The osmolarity and pH of this solution were adjusted to 310 mOsm l^{-1} and 7.4, respectively. When a Ca^{2+} free medium was required, $CaCl_2$ was omitted and replaced by equimolar $MgCl_2$. Dye loading was achieved by transferring the cells into a standard HBSS solution containing 1 mM Fura-2 AM (Calbiochem, Meudon, France) as described previously [25]. Δ[Ca^{2+} cyt] corresponds to an amplitude response ([Ca^{2+} cyt]max−[Ca^{2+} cyt]min).

2.8. Electrophysiological recordings

Macroscopic currents were recorded at room temperature (22 °C) by the whole-cell patch-clamp technique using an Axopatch 200B amplifier (Molecular Devices). The extracellular solution contained 150 mM NaCl, 6 mM KCl, 1.5 mM $CaCl_2$, 1 mM $MgCl_2$, and 10 mM HEPES, with pH adjusted to 7.4 with NaOH. The resistance of the patch pipettes fabricated from borosilicate glass capillaries (World Precision Instruments, Inc., Sarasota, FL) when filled with the intracellular solution was 2-3 MΩ for the whole cell recordings The internal solution contained 150 mM KCl, 5 mM EGTA, 10 mM HEPES, 3 mM magnesium-ATP, with pH adjusted to 7.2 with KOH. In the whole cell experiments, series resistance was compensated for by about 70%. Currents were filtered at 1 or 2 kHz and sampled at 10 kHz. For temperature control and solution exchange, the TC1-SL25 system (Bioscience Tools, San Diego, CA) was used with the temperature probe placed near the patch pipette tip. The system provided a temperature stability of at least 0.2 °C. Membrane current recordings obtained were analyzed and plotted using the pCLAMP 9 (Axon Instruments, Inc.) and Origin 5 software (Microcal Software Inc.).

2.9. Antibody production

Rabbit polyclonal antibody anti-hTRPV2 and anti-mTRPV2 were produced in the laboratory headed by Dr. Rassendren (CNRS UMR 5203, INSERM U661, Montpellier, France). The polypeptide ASEENYVPVQLLQS corresponding to 740–763 aa of the C-terminus sequence of the human TRPV2 channel (NM_016113) was injected into rabbit to produce a polyclonal antibody anti-hTRPV2. The polypeptide IDRDSGNPQPLVNAQ corresponding to 137–151 aa of the

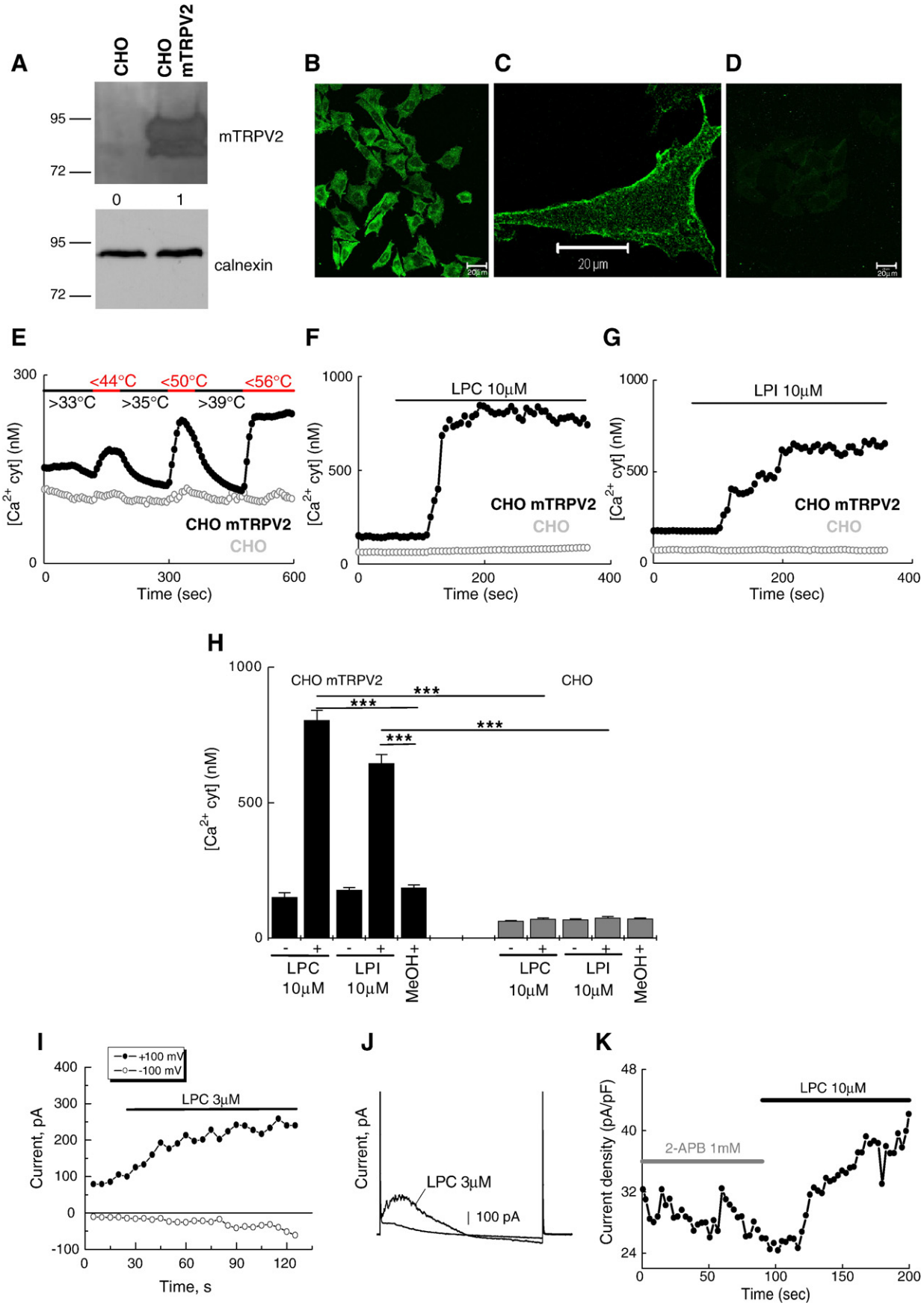
A
CHO
CHO mTRPV2
95
72
mTRPV2
0
1
95
72
calnexin
B
C
D
20 µm
E
<44°C
<50°C
<56°C
>33°C
>35°C
>39°C
[Ca2+ cyt] (nM)
CHO mTRPV2
CHO
Time (sec)
F
LPC 10µM
[Ca2+ cyt] (nM)
CHO mTRPV2
CHO
Time (sec)
G
LPI 10µM
[Ca2+ cyt] (nM)
CHO mTRPV2
CHO
Time (sec)
H
CHO mTRPV2
CHO
***
[Ca2+ cyt] (nM)
LPC 10µM
LPI 10µM
MeOH+
I
+100 mV
-100 mV
LPC 3µM
Current, pA
Time, s
J
Current, pA
LPC 3µM
100 pA
K
LPC 10µM
2-APB 1mM
Current density (pA/pF)
Time (sec)

mouse TRPV2 channel (NM_011706) was injected into rabbit to produce polyclonal antibody anti-mTRPV2.

2.10. Immunoblotting

After treatment the cells were rinsed with a NaCl solution (150 mM) and lysed in an ice-cold homogenizing buffer (pH 7.2) containing 20 mM PO_4Na_2K, 1% Triton X100, 1% sodium desoxycholate, 5 mM EDTA and a protease inhibitor cocktail (P8340, Sigma) for 30 min at 4 °C. Homogenates were cleared by centrifugation at 16,000 *g* for 10 min and the protein content in the supernatants was determined using the BCA method (Pierce, Chemical Co., Rockford, IL). 4 μg of total proteins were analyzed using 10% SDS-polyacrylamide gel electrophoresis. After the transfer onto a PVDF membrane using a semi-dry electroblotter, the membrane was cut into thin strips that were further processed for immunodetection. The strips were blocked in 5% non-fat dry milk in TBST (15 mM Tris buffer (pH 8), 140 mM NaCl, 0.05% Tween 20), washed three times, then incubated with a polyclonal anti-mTRPV2 antibody (rabbit, 1/250), or with a polyclonal anti-hTRPV2 antibody (rabbit, 1/250) as previously described [15], or with a polyclonal anti-GFP antibody (rabbit, 1/500 catalog no. AB3080P; Chemicon). After washing, blots were incubated for 1 h with the corresponding horseradish peroxydase-linked secondary antibody and processed for chemoluminescent detection (Pierce, Chemical Co., Rockford, IL) according to the manufacturer's instructions (Eastman Kodak Co., Rochester, NY). Membranes were reblotted twice with a monoclonal antibody anti-actin (mouse, 1/500 catalog no. MS-1295-P; Neomarkers), or with a monoclonal antibody anti-calnexin (mouse, 1/2000 catalog no. MAB 3126; Chemicon). The bands on the membrane were visualized using the enhanced chemiluminescence method (Pierce Biotechnologies Inc.). Densitometric analysis was performed using a Bio-Rad image acquisition system (Bio-Rad Laboratories).

2.11. Biotinylation assay

TRPV2 cell surface expression was analyzed in HEK293 cells as well as in the stable cell line CHO mTRPV2 transiently transfected (72 h) with hTRPV2-GFP. After treatment with LPC or LPI (data not shown) for 15 min, cells were washed twice with ice-cold PBS containing 1 mM $MgCl_2$ and 0.5 mM $CaCl_2$ (PBS-CM) and subjected to cell surface biotinylation as described previously [26]. Biotinylated proteins were precipitated using neutravidin-agarose beads (Pierce, Rockford, IL, USA) and eluted with SDS-PAGE loading buffer. TRPV2 expression analysis was analyzed by immunoblotting with antibody anti-mTRPV2 or anti-hTRPV2 as described in the Immunoblotting section above.

2.12. Migration protocol

PC3 nucleofected cells were seeded onto the top of Transwell® cell culture inserts with 8.0 μm pore size (Falcon), at a density of 30,000 cells per well (24-well format) in serum-free culture medium. Cells were stimulated to migrate across the filters by providing 10% fetal calf serum as a chemoattractant in the assay chambers beneath the inserts. After 2 h, almost two-thirds of the cells were adherent to each filter in the inserts. 10 μM LPC or LPI was then added to the upper chamber (or water as a control solvent). After 26 h incubation at 37 °C, non migratory cells were removed from the top of the filter by scraping, while cells that had migrated through the filter pores to the lower face of the inserts were fixed in 4% paraformaldehyde in PBS, and stained with Hoechst (5 mg/L in PBS). Cells under each filter were counted on five random examination fields (×200) using a Leica DMIRB inverted microscope. Data are expressed as means of 4 wells ± SEs.

2.13. Data analysis

Results are expressed as means ± SEM. Plots were produced using Origin5.0 (Microcal Software, Inc). *N* corresponds to a number of cells; *n* corresponds to a number of independent experiments. Each experiment was repeated at least three times. The Turkey–Kramer test was used for statistical comparison among means and differences. *—corresponds to $P<0.05$; **—corresponds to $P<0.01$; ***—corresponds to $P<0.005$. $P<0.05$ was considered as significant.

3. Results

3.1. Lysophospholipids activate TRPV2 channel

We have previously reported that the transient transfection of TRPV2 results in the high levels of its protein expression leading to cellular toxicity [10]. To avoid this problem, we have used a stable CHO cell line expressing mTRPV2 channel [10,15]. Prior to functional studies, we confirmed mTRPV2 protein expression by immunoblotting (Fig. 1A) and its plasma membrane localisation by immunofluorescence (Fig. 1B, C and D). The cytoplasmic $[Ca^{2+}]$ was measured by the microscopy-based single-cell imaging technique using the ratiometric Ca^{2+} indicator dye fura-2. To induce Ca^{2+} influx via mTRPV2 and to control the channel functionality, preheated solution was used (Fig. 1E).

Subsequently, we studied the effect of LPC and LPI on CHO-mTRPV2 cells. Application of 10 μM LPC and 10 μM LPI induced a sustained $[Ca^{2+}]_{cyt}$ increase after few minutes in CHO-mTRPV2 cells (Fig. 1F and G, mean time delay was 66 s ± 33 s for LPC and 72 s ± 24 s for LPI). Indeed, stimulation by LPC and LPI induced a $[Ca^{2+}]_{cyt}$ increase of 810 nM ± 35 nM and 646 nM ± 31 nM, respectively, in CHOmTRPV2 cells (Fig. 1H). Extracellular application of LPC activated an outwardly rectifying membrane current in CHOmTRPV2 cells (Fig. 1I, J), which by its biophysical properties was similar to I_{TRPV2} induced by 2-APB [15], thereby demonstrating that lysophospholipids are able to activate TRPV2 from the outside of the membrane. Moreover, 10 μM LPC induced potentiation on the activation of mTRPV2 current already pre-activated by 1 mM 2-APB (Fig. 1K). Different concentrations of LPC and LPI were examined by calcium imaging technique (see the dose effects of LPC and LPI which are presented in the supplementary data, Figs. 1 and 2, respectively). Of them, the lowest effective concentration of 10 μM was used in this study. LPC and LPI solvent (MeOH) had no effect on the cells (Fig. 1H).

To check if lysophospholipids could be a common activator for both mouse and human TRPV2 homologues, we tested LPC and LPI effects on HEK293 cells overexpressing hTRPV2. Thus, HEK293 cells were nucleofected with hTRPV2-GFP. The expression of hTRPV2-GFP channel was detected 72 h after nucleofection by GFP fluorescence using HEK-

Fig. 1. mTRPV2 is activated by LPC and LPI. (A) Immunoblotting of CHO-mTRPV2 cell lysates with the anti-mTRPV2 antibody showing two immunopositive bands: one glycosylated of 92 kDa and one not glycosylated of 83 kDa. The numbers indicated under the mTRPV2 panel are the relative integrative intensities of the bands. (B) Confocal images showing immuno-localisation of TRPV2 in CHO-mTRPV2 cells. (C) Higher magnification revealed the plasma membrane localisation of the channel, (D) CHO cells are used as a negative control. (E) Representative traces measured by Ca^{2+} imaging showing the effects of high temperatures (indicated by red bars) in CHO-mTRPV2 ($N=90$; $n=3$) and CHO control cells ($N=90$; $n=3$). (F) Representative traces measured by Ca^{2+} imaging showing the effect of LPC 10 μM in CHO mTRPV2 cells ($n=90$) versus CHO control cells ($N=90$; $n=3$). (G) Ca^{2+} imaging experiment showing the effect of LPI 10 μM in CHO mTRPV2 cells ($N=90$; $n=3$), not in CHO control cells ($N=90$; $n=3$). (H) Comparative graph showing maximal mean in response to LPC 10 μM ($N=90$; $n=3$), LPI 10 μM ($N=90$; $n=3$) and methanol (MeOH) vehicle ($N=90$; $n=3$) between CHO-mTRPV2 and CHO control cells. (I) Time courses of the current (measured at ±100 mV) changes in response to LPC (3 μM) ($n=10$) in CHO-mTRPV2 cells. Experiments shown were conducted at 22 °C. (J) Representative voltage ramp-derived I–V relationships demonstrating the activation of mTRPV2 current by LPC (3 μM). (K) Time courses of the current (measured at +100 mV) changes in response to LPC (10 μM) ($n=5$) after response to 2-APB 1 mM in CHO-mTRPV2 cells.

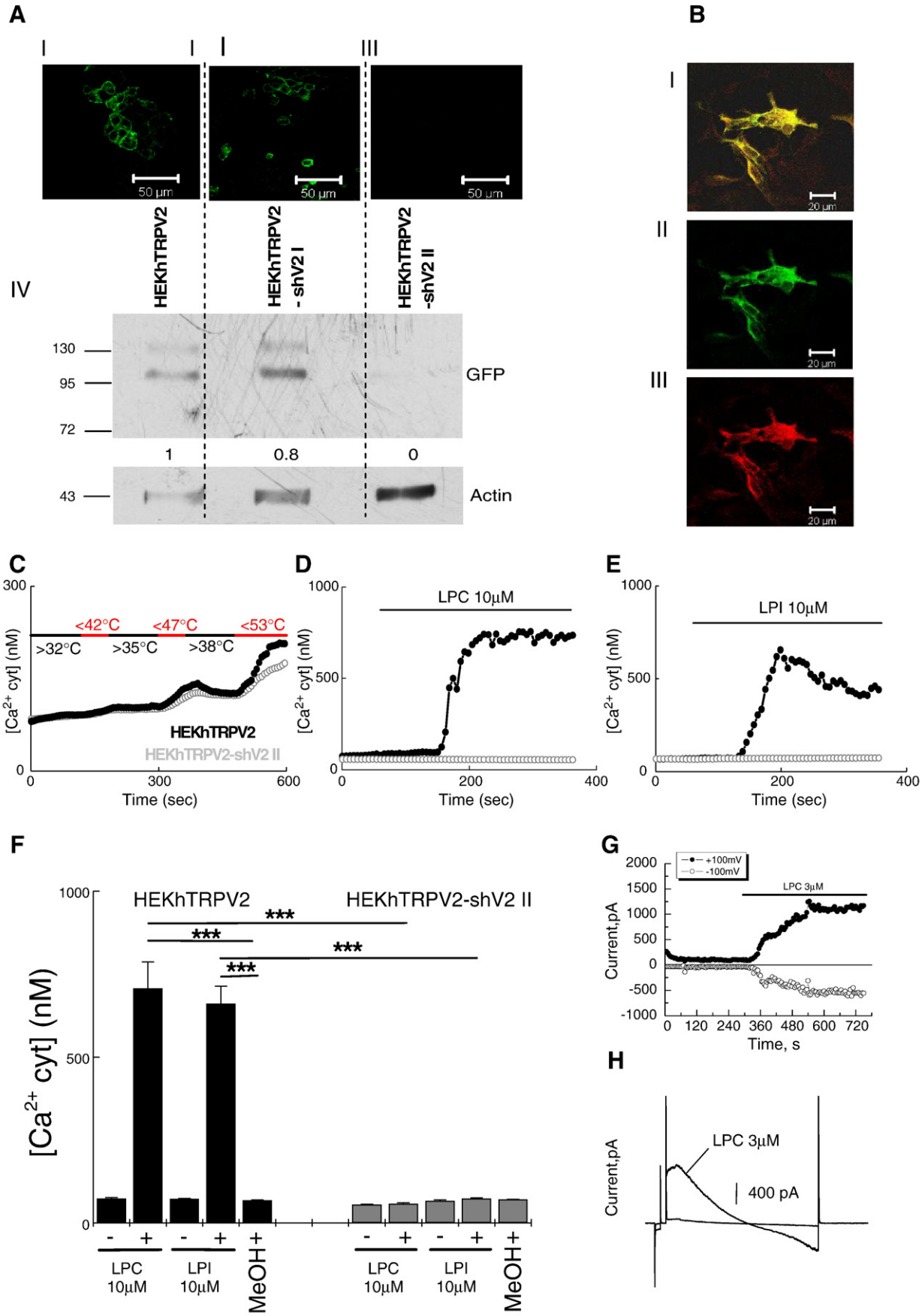
A
I
I
I
III
50 µm
50 µm
50 µm
HEKhTRPV2
HEKhTRPV2 - shV2 I
HEKhTRPV2 -shV2 II
IV
130
95
72
GFP
1
0.8
0
43
Actin
B
I
II
III
20 µm
20 µm
20 µm
C
300
<42°C
<47°C
<53°C
>32°C
>35°C
>38°C
[Ca2+ cyt] (nM)
HEKhTRPV2
HEKhTRPV2-shV2 II
0
300
600
Time (sec)
D
1000
LPC 10µM
[Ca2+ cyt] (nM)
500
0
200
400
Time (sec)
E
1000
LPI 10µM
[Ca2+ cyt] (nM)
500
0
200
400
Time (sec)
F
1000
HEKhTRPV2
HEKhTRPV2-shV2 II
***
***
***
***
[Ca2+ cyt] (nM)
500
0
- + - + +
LPC 10µM
LPI 10µM
MeOH
- + - + +
LPC 10µM
LPI 10µM
MeOH
G
2000
+100mV
-100mV
LPC 3µM
Current,pA
1500
1000
500
0
-500
-1000
0 120 240 360 480 600 720
Time, s
H
Current,pA
LPC 3µM
400 pA

Table 1
List of primers used for RT-PCR amplifications

	5′-forward-3′	5′-reverse-3′	Expected product size (bp)	Accession number
TRPV2	AAAGGGAACAGGTGCCAGTCA	TCCCACTGCTTGGTGCAAGCG	475	NM_016113.3
β-actin	CAGAGCAAGAGAGGCATCCT	GTTGAAGGTCTCAAACATGATC	210	NM_001101

hTRPV2 cells (Fig. 2A, I). In order to specifically reduce hTRPV2 expression, we used a co-nucleofection protocol with shRNA-TRPV2 I or II. TRPV2 expression was downregulated by 20% in shRNATRPV2 I (Fig. 2A, II) and by 100% in shRNA TRPV2 II (Fig. 2A, III) expressing cells. TRPV2 silencing was confirmed by immunoblotting with anti-GFP antibody. For other experiments, we used shRNA TRPV2 II since it has shown the highest TRPV2 silencing level (Fig. 2A, IV). Immuno-histochemical analysis of HEK293 cells nucleofected as described in Experimental Procedures confirmed that hTRPV2 is co-localised with a GFP protein (Fig. 2B, I). The GFP protein (Fig. 2B, II) was detected in hTRPV2-positive cells, with the intense intracellular labelling exactly overlapping the expression of this channel (Fig. 2B, III).

In Ca^{2+} imaging experiments, no difference was observed in $[Ca^{2+}]_{cyt}$ increased by high temperature. High temperature induced a $[Ca^{2+}]_{cyt}$ increase with a maximal amplitude of 206 nM±3 nM in HEKh-TRPV2 cells and 175±4 nM in HEK-hTRPV2-shTRPV2 II cells, respectively (Fig. 2C). The effects of 2-APB have been also investigated on calcium responses mediated by human TRPV2 channel by patch clamp, but any current was observed in HEKh-TRPV2 cells following 2-APB application (not shown; $n=4$). Therefore, high temperatures as well as 2-APB failed to activate the human homologue of TRPV2 [14].

However, 10 μM LPC (706 nM±79 nM; Fig. 2D, F) and 10 μM LPI (660 nM±53 nM; Fig. 2E, F) induced a $[Ca^{2+}]_{cyt}$ increase only in HEKh-TRPV2 cells, but not in HEKh-TRPV2-shTRPV2 II. Moreover, application of LPC (3 μM) in HEKh-TRPV2 cells induced a current (Fig. 2G, H) which was similar to that observed in CHOmTRPV2 cells (Fig. 1I, J).

3.2. Lysophospholipids chain length and composition define TRPV2 stimulation

Lysophospholipids consist of a polar head-group and an unsaturated chain of a fatty acid. LPC and LPI have choline and inositol head-groups, respectively. We therefore checked whether the head-groups and the unsaturated chain lengths exerted distinct effects on TRPV2 activity. We demonstrated that a mix of fatty acids had no effect on either mTRPV2 channel (Fig. 3A) or hTRPV2 channel (Fig. 3B). We have also shown that choline had no effect on CHOm-TRPV2 cells (Fig. 3A) nor on HEK-hTRPV2 cells (Fig. 3B). Additional lysophospholipids such as lysophosphatic acid (LPA) or Lysophosphatidylethanolamine (LPE) and sphingolipids such as Sphingosine-1-phosphate (S1P) have been examined. None of these had any significant effect on CHO-mTRPV2 cells (Fig. 3A, 9±2 nM for LPA, 59 nM±9 nM for S1P, 15 nM±9 nM for LPE and 662 nM±37 nM for LPC) nor on HEK-hTRPV2 cells (Fig. 3B, 3±1 nM for LPA, 36 nM±10 nM for S1P, 5 nM±2 nM for LPE and 631 nM±79 nM for LPC, respectively).

Thus, to stimulate the TRPV2 channel, lysophospholipids should exhibit a precise combination of a head-group and a side chain. We have demonstrated that chain lengths greater than 12 carbons are needed to stimulate mTRPV2 (6 nM±4 nM for LPC C6:0; 7 nM±2 nM for LPC C12:0; 73 nM±8 nM for LPC C14:0; 573 nM±43 nM for LPC C16:0; 737 nM±39 nM for LPC C18:0; 692 nM±34 nM for LPC C18:1; and 744 nM±33 nM for LPC CTL in CHO-mTRPV2; Fig. 3C) as well as hTRPV2 (1 nM±6 nM for LPC C6:0; 3 nM±1 nM for LPC C12:0; 61 nM±13 nM for LPC C14:0; 454 nM±59 nM for LPC C16:0; 585 nM±70 nM for LPC C18:0; 529 nM±33 nM for LPC C18:1; and 628 nM±38 nM for LPC CTL in HEKh-TRPV2; Fig. 3D).

3.3. LPC induces Ca^{2+} influx through TRPV2 via the G-protein and the PI3,4K pathways

In order to discriminate the origin of Ca^{2+} increase induced by lysophospholipids, we tested LPC and LPI (data not shown) on CHO-mTRPV2 and HEK-hTRPV2 without Ca^{2+} in the extracellular medium (0 Ca^{2+}). LPC did not induce significant depletion of endoplasmic reticulum (ER) Ca^{2+} stores in CHO-mTRPV2 (Fig. 4A, C 61 nM±27 nM) and HEK-hTRPV2 (Fig. 4B, C 10 nM±3 nM) cells. Application of 2 mM Ca^{2+} (2Ca^{2+}) in the extracellular medium resulted in a massive Ca^{2+} entry with an amplitude of 683 nM±58 nM (Fig. 4C) in CHO-mTRPV2 and of 530 nM±30 nM (Fig. 4C) in HEK-hTRPV2 cells. Thus lysophospholipids activate both mTRPV2 and hTRPV2 channels presented in the plasma membrane (Figs. 1B, C and 2Aa) inducing a Ca^{2+} entry into the cells.

It is known that LPC acts on various intracellular signalling pathways [27]. In order to understand the activation mechanism of LPC, we used different inhibitors of intracellular signalling pathways. 10 μM U73122, a PLC inhibitor, had no effect on the LPC response (Fig. 4D). The pretreatment with 50 μM PI3,4K inhibitor wortmannin (Fig. 4D) for 15 minutes had a weak effect on Ca^{2+} entry induced by LPC 10 μM (521 nM±31 nM) in CHO-mTRPV2 cells. However, pretreatment with wortmannin 150 μM (the dose-effect curves of wortmannin are presented in the supplementary data, Fig. 5), or with another PI3,4K inhibitor LY294002 50 μM for 15 min, respectively, drastically inhibited the LPC effect (Fig. 4D) (15 nM±5 nM) or partially inhibited the LPC effect (Fig. 4D) (141 nM±26 nM) on CHO-mTRPV2 cells. In order to check whether LPC effect is mediated by G-protein, we used pertussis toxin (PTX), an inhibitor of Gi and Go proteins [28]. Pretreatment with 250 ng/ml PTX for 12 h abolished the Ca^{2+} entry induced by LPC on CHO-mTRPV2 (Fig. 4D 7 nM±3 nM). We also tested the effects of the same molecules on the hTRPV2 channel. Pretreatment of HEK-hTRPV2 cells with 50 μM LY294002 for 15 min or with PTX 250 ng/ml for 12 h also blocked the Ca^{2+} entry induced by LPC (Fig. 4E, 117 nM±5 nM and 3 nM±1 nM, respectively). Therefore, the activation of the TRPV2 channel by LPC is mediated by G-proteins and the PI3,4K pathway.

Fig. 2. LPC and LPI activate hTRPV2 channel. (A) Cells nucleofected with hTRPV2-GFP and the pSilencer empty vector (HEK-hTRPV2) (I) are analyzed 72 h later for GFP fluorescence emission. Cells co-nucleofected with hTRPV2-GFP and shRNA TRPV2 I (HEKhTRPV2-shV2 I) (II). GFP fluorescence is totally abolished when cells are nucleofected (72 h) with hTRPV2/GFP+shRNA TRPV2 II (HEKhTRPV2-shV2 II) (III). Immunoblotting of HEK-hTRPV2, HEK-hTRPV2shV2 I and II cell lysates with the anti-GFP antibody showing hTRPV2 expression 72 h after nucleofection. The numbers indicated under the GFP panel are the relative integrative intensities of the bands. (IV). (B) Confocal images showing (I) co-localisation for GFP (II) and hTRPV2 (III) detected by anti-hTRPV2 antibody. (C) Representative traces measured by Ca^{2+} imaging showing the effect of high temperatures (indicated by red bars) in HEK-hTRPV2 ($N=90$; $n=3$) and HEK-hTRPV2-shV2 II control cells ($N=90$; $n=3$). (D) Representative traces measured by Ca^{2+} imaging showing the effect of LPC 10 μM in HEK-hTPV2 cells ($N=60$; $n=3$), and in HEK-hTRPV2-shV2 II control cells ($N=60$; $n=3$). (E) Ca^{2+} imaging experiment showing the effect of LPI 10 μM in HEK-hTPV2 cells ($N=60$; $n=3$), and in HEK-hTRPV2-shV2 II control cells ($N=60$; $n=3$). (F) Comparative graph showing maximal mean in response to LPC 10 μM ($N=60$; $n=3$), LPI 10 μM ($N=60$; $n=3$) and methanol (MeOH) vehicle ($N=60$; $n=3$) between HEK hTRPV2 and HEK-hTRPV2 shV2 II cells. (G) Time courses of the current (measured at ±100 mV) changes in response to LPC (3 μM) in HEK-hTRPV2 cells ($n=7$). (H) Representative voltage ramp-derived I–V relationships demonstrating the activation of hTRPV2 current by LPC (3 μM).

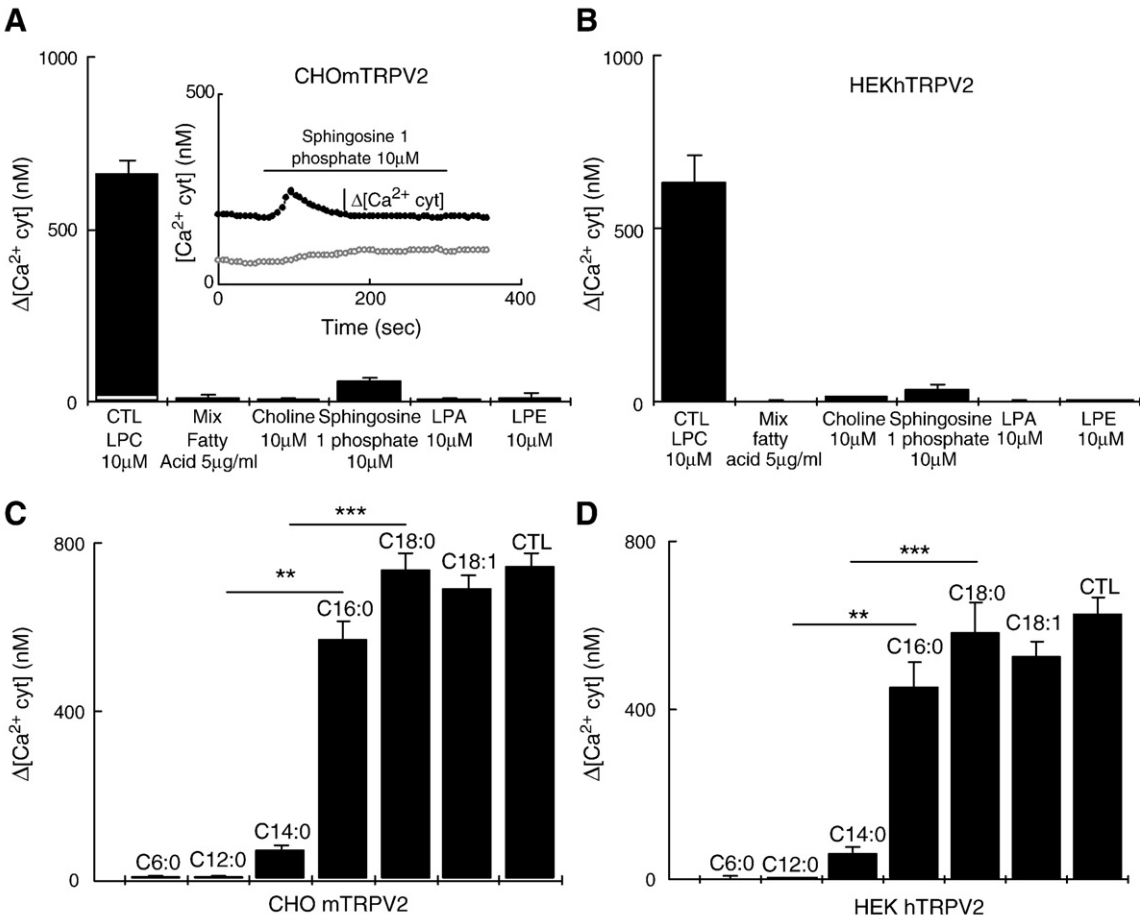

Fig. 3. Screening of various lysophospholipids on TRPV2 activity. (A) Comparative graph obtained by Ca^{2+} imaging showing maximal mean ($\Delta[Ca^{2+}$ cyt]) in response to LPC ($N=90$; $n=3$) as control, a mix of fatty acids ($N=90$; $n=3$), choline ($N=90$; $n=3$), S1P ($N=90$; $n=3$), LPA ($N=90$; $n=3$) and LPE ($N=60$; $n=3$) in CHO-mTRPV2 cells. (B) Ca^{2+} imaging experiment showing maximal mean in response ($\Delta[Ca^{2+}$ cyt]) to LPC ($N=60$; $n=3$) as control, a mix of fatty acids ($N=60$; $n=3$), choline ($N=60$; $n=3$), S1P ($N=60$; $n=3$), LPA ($N=60$; $n=3$) and LPE ($N=60$; $n=3$) in HEK-hTRPV2 cells. (C) Comparative graph showing $\Delta[Ca^{2+}$ cyt] in response to LPC CTL 10 μM ($N=60$, $n=3$), LPC C18:1 ($N=60$, $n=3$), LPC C18:0 ($N=60$; $n=3$), LPC C16:0 ($N=60$; $n=3$), LPC C14:0 ($N=60$; $n=3$), LPC C12:0 ($N=60$; $n=3$) and LPC C6:0 ($N=60$; $n=3$) in CHO-mTRPV2 cells. (D) Ca^{2+} imaging experiment showing $\Delta[Ca^{2+}$ cyt] in response to LPC CTL 10 μM ($N=60$, $n=3$), LPC C18:1 ($N=60$, $n=3$), LPC C18:0 ($N=60$; $n=3$), LPC C16:0 ($N=60$; $n=3$), LPC C14:0 ($N=60$; $n=3$), LPC C12:0 ($N=60$; $n=3$) and LPC C6:0 ($N=60$; $n=3$) in HEK-hTRPV2 cells. All lysophospholipids molecules were used at 10 μM concentration.

3.4. LPC induces TRPV2 translocation to the plasma membrane

In order to check if the Ca^{2+} influx via TRPV2 channel is due to an increased plasma membrane channel expression, we performed cell surface biotinylation (Fig. 5A, $n=3$). When cells were stimulated with LPC, the amount of mTRPV2 expressed in the biotinylated fraction markedly increased (Fig. 5A). As PTX and LY294002 inhibited the Ca^{2+} entry induced by LPC, we studied their effect on mTRPV2 translocation. Pretreatment with 250 ng/ml PTX only or with 50 μM LY294002 had a weak effect, but these pretreatments abolished the LPC effect on TRPV2 plasma membrane translocation (Fig. 5A). The cell surface expression of hTRPV2 was increased when 10 μM LPC was applied in HEK-hTRPV2 (Fig. 5B, $n=3$).

3.5. LPC and LPI stimulate endogenous TRPV2 and induce cell migration

Semi-quantitative RT-PCR and immunoblotting analysis of the human prostate cancer cell PC3 line revealed a high level of TRPV2 expression (Fig. 6A, B). TRPV2 silencing with shRNA TRPV2 I and II (PC3 shV2 I and II) abolished the channel expression both on mRNA (Fig. 6A) and protein levels (Fig. 6B) compared to PC3 nucleofected with the empty pSilencer vector (PC3 pSil cells).

By using Ca^{2+} imaging, we have demonstrated that 10 μM LPC and 10 μM LPI induce a Ca^{2+} entry in PC3 pSil cells, but not in PC3 shV2 I and II (Fig. 6C and D). However, PC3 cells expressed other TRP channels such as TRPV1, which is known to be sensitive to lysophospholipids [17,29,30]. In order to ensure that LPC and LPI effects were specific for TRPV2 channel, we applied 10 μM capsazepin, an inhibitor of TRPV1. In the presence of capsazepin, LPC and LPI still induced an increase in the Ca^{2+} influx which was abolished with the TRPV2 silencing. This proves that LPC and LPI act on the endogenous TRPV2 channel, expressed in PC3 cells, providing Ca^{2+} entry. It has been shown previously that lysophospholipids induced PC3 cell migration [31–33]. We have demonstrated using a migration protocol that basal cell migration was decreased in PC3 shTRPV2 I and in PC3 shTRPV2 II cells compared to PC3 pSil cells (89±5 cells for PC3 pSil cells, 59±10 cells for PC3 shTRPV2 I cells, 58±12 cells for PC3 shTRPV2 II cells, Fig. 6E). Moreover, we have shown that both 10 μM LPI and LPC induce an increase in cell migration of PC3 pSil cells (Fig. 6E, 103±4 cells for LPI, 108±6 cells for LPC, compared to control H_2O condition 89±5 cells). However, lysophospholipid effects on cell migration are totally abolished in PC3 shTRPV2 I cells (52±5 cells for LPI and 48±7 cells for LPC) and in PC3 shTRPV2 II cells (respectively 51±5 cells for LPI and 43±8 cells for LPC). We have demonstrated that a higher concentration (20 μM) of LPC and LPI induced a decrease of PC3 pSil cell migration by 10±12% and 55±12% respectively compared to control H_2O condition (Fig. 6F). Moreover, we have shown that pretreatment with LY294002 (50 μM) decreased cell migration by 25±14% compared to control H_2O

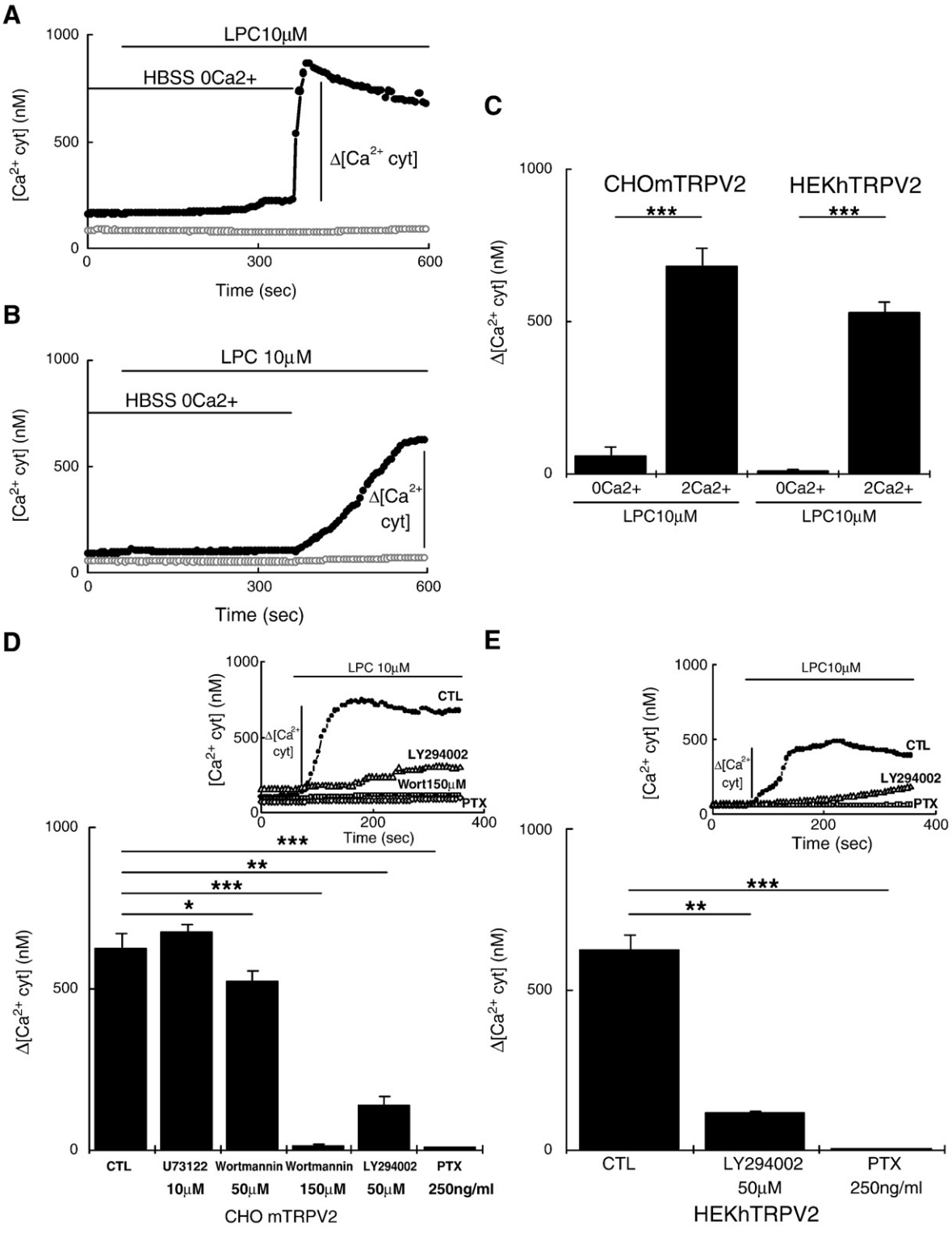

Fig. 4. Basic characterization of TRPV2 by Ca^{2+} imaging. (A) LPC induced a slight depletion of Ca^{2+} store in Ca^{2+} free condition (HBSS $0Ca^{2+}$) and a strong Ca^{2+} influx in presence of 2 mM Ca^{2+} in CHOmTRPV2 (N=60; n=3), (B) as for HEK-hTRPV2 cells (N=60; n=3). LPC has no effect on CHO or HEK control cells (A, B) (N=60; n=3 per condition). (C) Comparative graph showing $\Delta[Ca^{2+}$ cyt] in response to LPC in the absence of Ca^{2+} (HBSS $0Ca^{2+}$) and in the presence of 2 mM Ca^{2+} in CHO-mTRPV2 and in HEK-hTRPV2 cells (N=60; n=3 per condition). (D) Ca^{2+} imaging experiment showing that pretreatment with 10 μM U73122, 30 min, has no effect on the amplitude ($\Delta[Ca^{2+}$ cyt]) of LPC response but pretreatment with 50 μM wortmannin, 15 min, has a weak effect on this amplitude. Moreover, pretreatment with wortmannin 150 μM or with 50 μM LY294002 for 15 min drastically diminished the amplitude of the response induced by LPC in CHO-mTRPV2 (N=60; n=3). The characteristic traces are shown in the inserted panel (N=60; n=3 per condition). Pretreatment with PTX 250 ng/ml overnight abolished LPC response in CHO-mTRPV2 cells (N=60; n=3 per condition). (E) Comparative graph showing that pretreatment with 250 ng/ml PTX overnight or with 50 μM LY294002 15 min, totally inhibited the amplitude ($\Delta[Ca^{2+}$ cyt]) of LPC response in HEK-hTRPV2 cells. The characteristic traces are shown in the inserted panel (N=60; n=3 per condition).

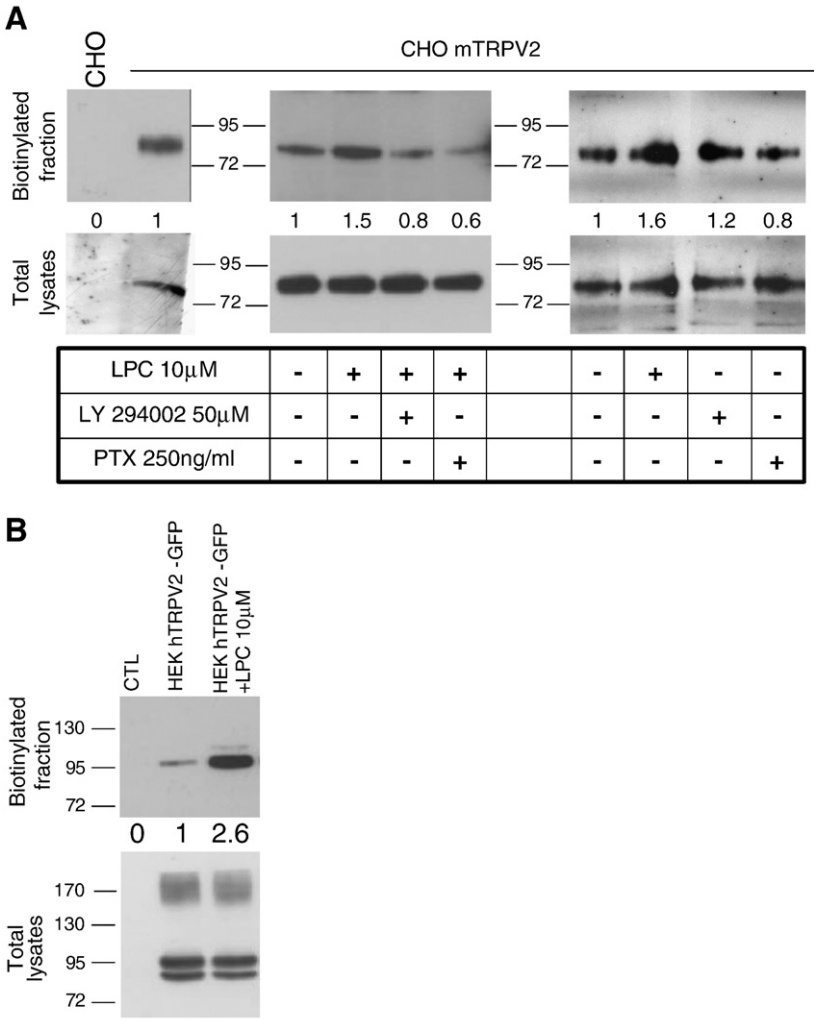

Fig. 5. LPC induces translocation of TRPV2 to the plasma membrane. (A) Immunoblotting with the anti-mTRPV2 antibody showing increase in mTRPV2 expression in the biotinylated fraction after LPC (10 μM) application on CHO-mTRPV2 cells ($n=3$). This increase was abolished by pretreatment with 50 μM LY294002 or 250 ng/ml PTX (overnight). Pretreatment only with 50 μM LY294002 or 250 ng/ml PTX (overnight) has a weak effect. The numbers indicated under the biotinylated fraction panel are the relative integrative intensities of the bands. (B) Immunoblotting with anti-hTRPV2 antibody showing increase in hTRPV2 expression in biotinylated fraction from 10 μM LPC treatment ($n=3$). The numbers indicated under the biotinylated fraction panel are the relative integrative intensities of the bands.

condition and also inhibited by 60% the effect of LPC on PC3 cell migration (Fig. 6G).

4. Discussion

In our study we investigated phospholipids as potential physiological activators of TRPV2 channels and we found that lysophospholipids, LPC and LPI, are able to stimulate mTRPV2 as well as hTRPV2. More precisely, LPC and LPI generated a Ca^{2+} entry by inducing the translocation of TRPV2 protein to the plasma membrane. Our results showed that activation and translocation of TRPV2 by lysophospholipids are mediated by G proteins and P13,4K pathways. Moreover, we have demonstrated that in TRPV2 expressing prostate cancer PC3 cells, LPC and LPI increased cell migration, while TRPV2 silencing drastically diminished the lysophospholipid-induced effect.

LPC and LPI stimulated both murine and human TRPV2 homologues, suggesting common activation mechanisms for mTRPV2 and hTRPV2. However, 2-APB and high temperatures stimulated mTRPV2, but not hTRPV2. Such divergence in modes of activation between the human and murine TRPV2 homologues has been previously observed by Neeper et al. [14]. The authors suggest that both the NH2- and COOH-terminal regions appear to be important for channel activation by 2-APB and high temperature [14].

LPC and LPI are widely found in biological systems and are considered to have a broad range of physiological and pathological effects [34–38]. We have shown that lysophospholipid application induces a rapid $[Ca^{2+}]_{cyt}$ increase. Importantly, our results show that TRPV2 activation depends on the length of the unsaturated chain of the fatty acid and, moreover, that lysophospholipids need a specific combination of head-group composition and side chain length to stimulate the TRPV2 channel.

To date, there are two main hypotheses explaining lysophospholipidic actions: (i) indirect action via a receptor for the LPA or the sphingosine [39]; (ii) direct action (as was suggested for the LPC effect on the TRPC5 channel [16,40]). Indeed, TRPC5 was considered as a direct sensor of lysophospholipids, a lipid ionotropic receptor. However, apparently in our case, lysophospholipid stimulation can be mechanistically attributed to signalling through specific G protein-coupled receptors. Lysophospholipids do not directly activate TRPV2 channels like a lipid ionotropic receptor. That is probably why we observed a Ca^{2+} increase induced by LPC or LPI via TRPV2 channel after some delay. The stimulatory effect of lysophospholipids on TRPV2 should be distinguished from those of 2-APB and high temperature

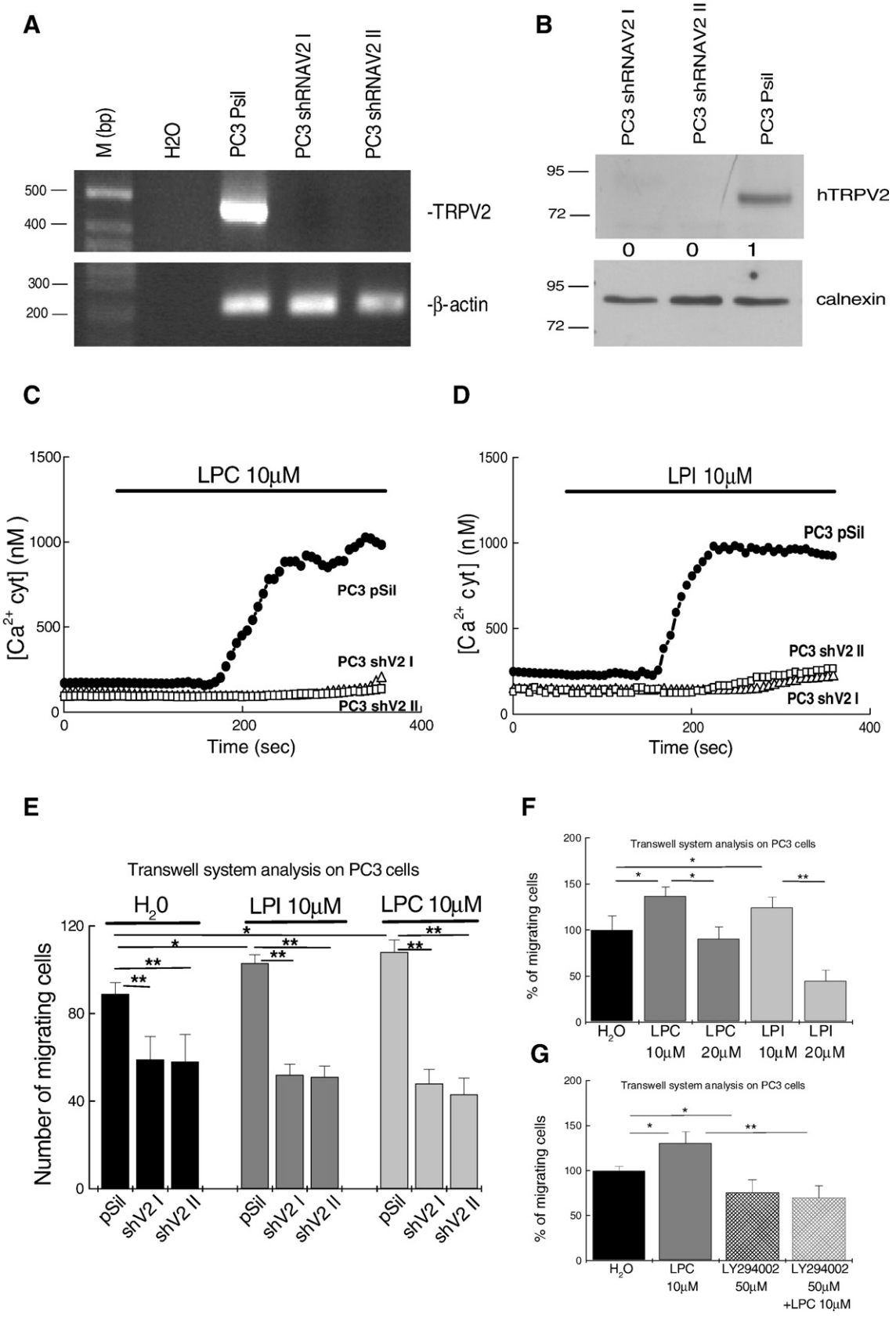

Fig. 6. LPC effects on the cell migration of the prostate cancer cell line PC3. (A) Silencing of TRPV2 expression in human prostate PC3 cells nucleofected with shTRPV2 I or II (PC3 shTRPV2 I or II) or empty vector (PC3 pSil). (B) Immunoblotting with antibody anti hTRPV2 showing that expression of TRPV2 protein in PC3 shTRPV2 I or II cells is abolished compared to PC3 pSil cells. The numbers indicated under the hTRPV2 panel are the relative integrative intensities of the bands. (C) 10 μM LPC induces cytoplasmic Ca^{2+} increase in PC3 pSil, but not in PC3 shTRPV2 I or II cells (N=90; n=3 per condition). (D) 10 μM LPI induces cytoplasmic Ca^{2+} in PC3 pSil, but not in PC3 shTRPV2 I or II cells (N=90; n=3 per condition). (E) 10 μM LPC and/or LPI induces cell migration increase in PC3 pSil. Cell migration in control are reduced in PC3 shTRPV2 I or II cells (n=3). Increases of cell migration induced by LPC and LPI are abolished in PC3 shTRPV2 I or II cells (n=3), (F) or by a higher concentration (20 μM) of LPC and/or LPI in PC3 pSil cells (n=3). (G) Pretreatment with 50 μM LY294002 decreased PC3 cell migration and abolished effect of LPC on those cells (n=3).

(on both NH2- and COOH- terminal regions), since LPC was able to potentialise mTRPV2 current already activated by 2-APB.

Our data suggest that lysophospholipids act on TRPV2 channels by the PI3,4K pathway, inducing the translocation of the channel to the plasma membrane. It is known that lysophospholipids could activate PI3,4K [39] and it has been suggested that these kinases are involved in TRPV2 activation [10]. Moreover, it has been shown that the chemotactic peptide fMetLeuPhe, a potent inducer of leucocyte chemotaxis and a macrophage activator, induces translocation of the TRPV2 channel via the PI3K pathway in macrophages [8]. However, the results on TRPV2 translocation towards the plasma membrane seem to be a controversial issue [41]. Indeed, it has been suggested that PI3K promotes TRPV2 activity independently of the channel translocation to the plasma membrane [10]. Furthermore, wortmannin and LY294002 at high concentrations were shown to inhibit the PI4K pathway [42,43]. Therefore, the insertion of TRPV2 into the plasma membrane could be regulated by PI4K and not by PI3K. It is important to note that the optimal specificity of the pharmacological agents may always be in question, therefore other tools such as siRNAs, mutants, or more specific pharmacological agents should be considered. In addition, a TRPV2 partner called recombinase gene activator protein (RGA) has recently been identified by an interaction trap screening. The binding of RGA to TRPV2 promotes its surface expression, in a protein kinase A-dependent way [41]. Finally, it has been proposed that Ca^{2+} could be involved in such a dynamic regulation of TRPV2 [44] by promoting the channel's activity and therefore Ca^{2+} influx. This suggests that other intracellular pathways could be involved in TRPV2 plasma membrane expression. It should be noted that the heterogeneity in the kinetics of $[Ca^{2+}]i$ increase following lysophospholipid application has been observed in our study (Fig. 4A,B). This finding could be explained by the differential amount of TRPV2 presented in the plasma membrane before the translocation stimulated by lysophospholipids.

We also demonstrate that LPC and LPI generate Ca^{2+} influx in the human prostate cancer cell line PC3 which expresses TRPV2 endogenously. It has been suggested that lysophospholipids are significant actors in tumour development, since they stimulate angiogenesis, growth, survival and migration of malignant cells from various origins [31–33] such as the ovary or the prostate [45,46]. Lysophospholipids were reported to be present in the micromolar range in these tissues [34,35] corresponding to the concentration which in our study was effective to induce calcium entry and to stimulate migration of cancer cells. However, high concentrations of lysophospholipids seemed to be cytotoxic. Recently, it has been shown that TRPM8 channels cloned from human prostate and known to be involved in prostate tumour development are also activated by lysophospholipids, acting as endogenous ligands of the channel [17].

TRPV2 is a physiological sensor of hot temperatures [47]. However, temperature alone is unlikely to account for activation of TRPV2 in all tissues [48]. TRPV2 is also expressed in non-neuronal cells such as the prostate [6] or human blood cells, suggesting that, in addition to its role as a noxious heat sensor [47], this channel certainly encompasses other cellular functions [49]. Previously, TRPV2 activation has been shown to be involved in macrophage cell migration [8]. The authors demonstrated that the chemotactic peptide fMetLeuPhe induces the migration of macrophages and that this migration is linked to the translocation of the TRPV2 channel via PI3K pathway. In accordance with these findings, our results on human prostate cancer cells strongly suggest TRPV2 as being a significant actor in cancer cell migration. Indeed, silencing with shRNA TRPV2 or inhibition of PI3,4K pathway abolished the stimulatory effect of lysophospholipids on both calcium entry and migration.

It is important to note that neurons and non-neuronal cells hardly ever experience the high temperatures which are generally considered to stimulate TRPV2 (>53 °C). Endogenous modulators, such as lysophospholipids, could lower the temperature threshold so that TRPV2 can operate at physiological body temperatures. In conclusion, these lipid modulators could therefore have two roles: setting the temperature sensitivity of heat receptors in neurons and regulating cell migration in non-neuronal tissues. Considering that cancer cell migration remains one of the less understood processes leading to cancer progression and that currently there is no treatment specifically targeting migrating cells, our findings provide new insight into the role of TRPV2 in cancer progression and may be of great importance in developing new therapeutic strategies.

Acknowledgments

This study was supported by grants from the Ministère de l'Education Nationale, ARC (Association pour la Recherche sur le Cancer), INSERM (Institut National de la Santé et de la Recherche Médicale), Ligue Nationale Contre le Cancer and European Molecular Biology Organization long-term fellowship ALTF-161-2006. The authors would like to thank Morad Roudbaraki for primers design, Loic Lemmonier for helpful advice and assistance, and Etienne Dewailly for his technical assistance. The authors declare that there is no conflict of interest that would prejudice the impartiality of this scientific work.

Appendix A. Supplementary data

Supplementary data associated with this article can be found, in the online version, at doi:10.1016/j.bbamcr.2009.01.003.

References

[1] M.J. Berridge, M.D. Bootman, H.L. Roderick, Calcium signalling: dynamics, homeostasis and remodelling, Nat. Rev., Mol. Cell Biol. 4 (2003) 517–529.
[2] A. Ferrer-Montiel, C. Garcia-Martinez, C. Morenilla-Palao, N. Garcia-Sanz, A. Fernandez-Carvajal, G. Fernandez-Ballester, R. Planells-Cases, Molecular architecture of the vanilloid receptor. Insights for drug design, Eur. J. Biochem. 271 (2004) 1820–1826.
[3] S.P. Alexander, A. Mathie, J.A. Peters, Guide to Receptors and Channels, 2nd edition (2007 Revision), Br. J. Pharmacol. 150 (Suppl. 1) (2007) S1.
[4] K. Venkatachalam, C. Montell, TRP channels, Annu. Rev. Biochem. 76 (2007) 387–417.
[5] V. Flockerzi, An introduction on TRP channels, Handb. Exp. Pharmacol. (2007) 1–19.
[6] T. Kowase, Y. Nakazato, O.H. Yoko, A. Morikawa, I. Kojima, Immunohistochemical localization of growth factor-regulated channel (GRC) in human tissues, Endocr. J. 49 (2002) 349–355.
[7] S. Bang, K.Y. Kim, S. Yoo, S.H. Lee, S.W. Hwang, Transient receptor potential V2 expressed in sensory neurons is activated by probenecid, Neurosci. Lett. 425 (2007) 120–125.
[8] M. Nagasawa, Y. Nakagawa, S. Tanaka, I. Kojima, Chemotactic peptide fMetLeuPhe induces translocation of the TRPV2 channel in macrophages, J. Cell. Physiol. 210 (2007) 692–702.
[9] M. Kanzaki, Y.Q. Zhang, H. Mashima, L. Li, H. Shibata, I. Kojima, Translocation of a calcium-permeable cation channel induced by insulin-like growth factor-I, Nat. Cell Biol. 1 (1999) 165–170.
[10] A. Penna, V. Juvin, J. Chemin, V. Compan, M. Monet, F.A. Rassendren, PI3-kinase promotes TRPV2 activity independently of channel translocation to the plasma membrane, Cell Calcium 39 (2006) 495–507.
[11] Y. Iwata, Y. Katanosaka, Y. Arai, K. Komamura, K. Miyatake, M. Shigekawa, A novel mechanism of myocyte degeneration involving the Ca^{2+}-permeable growth factor-regulated channel, J. Cell Biol. 161 (2003) 957–967.
[12] K. Muraki, Y. Iwata, Y. Katanosaka, T. Ito, S. Ohya, M. Shigekawa, Y. Imaizumi, TRPV2 is a component of osmotically sensitive cation channels in murine aortic myocytes, Circ. Res. 93 (2003) 829–838.
[13] H.Z. Hu, Q. Gu, C. Wang, C.K. Colton, J. Tang, M. Kinoshita-Kawada, L.Y. Lee, J.D. Wood, M.X. Zhu, 2-aminoethoxydiphenyl borate is a common activator of TRPV1, TRPV2, and TRPV3, J. Biol. Chem. 279 (2004) 35741–35748.
[14] M.P. Neeper, Y. Liu, T.L. Hutchinson, Y. Wang, C.M. Flores, N. Qin, Activation properties of heterologously expressed mammalian TRPV2: Evidence for species dependence, J. Biol. Chem. 282 (2007) 15894–15902.
[15] V. Juvin, A. Penna, J. Chemin, Y.L. Lin, F.A. Rassendren, Pharmacological characterization and molecular determinants of the activation of TRPV2 channel orthologs by 2-aminoethoxydiphenyl borate, Mol. Pharmacol. 72 (2007) 1258–1268.
[16] P.K. Flemming, A.M. Dedman, S.Z. Xu, J. Li, F. Zeng, J. Naylor, C.D. Benham, A.N. Bateson, K. Muraki, D.J. Beech, Sensing of lysophospholipids by TRPC5 calcium channel, J. Biol. Chem. 281 (2006) 4977–4982.

[17] F. Vanden Abeele, A. Zholos, G. Bidaux, Y. Shuba, S. Thebault, B. Beck, M. Flourakis, Y. Panchin, R. Skryma, N. Prevarskaya, Ca^{2+}-independent phospholipase A2-dependent gating of TRPM8 by lysophospholipids, J. Biol. Chem. 281 (2006) 40174–40182.
[18] C.D. Benham, J.B. Davis, A.D. Randall, Vanilloid and TRP channels: a family of lipid-gated cation channels, Neuropharmacology 42 (2002) 873–888.
[19] A. Tokumura, Physiological and pathophysiological roles of lysophosphatidic acids produced by secretory lysophospholipase D in body fluids, Biochim. Biophys. Acta 1582 (2002) 18–25.
[20] V.S. Kamanna, B.V. Bassa, S.H. Ganji, D.D. Roh, Bioactive lysophospholipids and mesangial cell intracellular signaling pathways: role in the pathobiology of kidney disease, Histol. Histopathol. 20 (2005) 603–613.
[21] K.S. Park, M.K. Kim, H.Y. Lee, S.D. Kim, S.Y. Lee, J.M. Kim, S.H. Ryu, Y.S. Bae, S1P stimulates chemotactic migration and invasion in OVCAR3 ovarian cancer cells, Biochem. Biophys. Res. Commun. 356 (2007) 239–244.
[22] A. Pebay, C.S. Bonder, S.M. Pitson, Stem cell regulation by lysophospholipids, Prostaglandins Other Lipid Mediat. 84 (2007) 83–97.
[23] S. Thebault, L. Lemonnier, G. Bidaux, M. Flourakis, A. Bavencoffe, D. Gordienko, M. Roudbaraki, P. Delcourt, Y. Panchin, Y. Shuba, R. Skryma, N. Prevarskaya, Novel role of cold/menthol-sensitive transient receptor potential melastatine family member 8 (TRPM8) in the activation of store-operated channels in LNCaP human prostate cancer epithelial cells, J. Biol. Chem. 280 (2005) 39423–39435.
[24] G. Bidaux, M. Flourakis, S. Thebault, A. Zholos, B. Beck, D. Gkika, M. Roudbaraki, J. L. Bonnal, B. Mauroy, Y. Shuba, R. Skryma, N. Prevarskaya, Prostate cell differentiation status determines transient receptor potential melastatin member 8 channel subcellular localization and function, J. Clin. Invest. 117 (2007) 1647–1657.
[25] S. Humez, M. Monet, G. Legrand, G. Lepage, P. Delcourt, N. Prevarskaya, Epidermal growth factor-induced neuroendocrine differentiation and apoptotic resistance of androgen-independent human prostate cancer cells, Endocr.-Relat. Cancer 13 (2006) 181–195.
[26] D. Gkika, C.N. Topala, Q. Chang, N. Picard, S. Thebault, P. Houillier, J.G. Hoenderop, R.J. Bindels, Tissue kallikrein stimulates Ca(2+) reabsorption via PKC-dependent plasma membrane accumulation of TRPV5, EMBO J. 25 (2006) 4707–4716.
[27] X. Wang, Lipid signaling, Curr. Opin. Plant Biol. 7 (2004) 329–336.
[28] P.R. Albert, L. Robillard, G protein specificity: traffic direction required, Cell. Signal. 14 (2002) 407–418.
[29] F. Ye, P.Y. Deng, D. Li, D. Luo, N.S. Li, S. Deng, H.W. Deng, Y.J. Li, Involvement of endothelial cell-derived CGRP in heat stress-induced protection of endothelial function, Vasc. Pharmacol. 46 (2007) 238–246.
[30] D.A. Andersson, M. Nash, S. Bevan, Modulation of the cold-activated channel TRPM8 by lysophospholipids and polyunsaturated fatty acids, J. Neurosci. 27 (2007) 3347–3355.
[31] F. Hao, M. Tan, X. Xu, J. Han, D.D. Miller, G. Tigyi, M.Z. Cui, Lysophosphatidic acid induces prostate cancer PC3 cell migration via activation of LPA(1), p42 and p38alpha, Biochim. Biophys. Acta 1771 (2007) 883–892.
[32] G.V. Raj, J.A. Sekula, R. Guo, J.F. Madden, Y. Daaka, Lysophosphatidic acid promotes survival of androgen-insensitive prostate cancer PC3 cells via activation of NF-kappaB, Prostate 61 (2004) 105–113.
[33] A. Picascia, R. Stanzione, P. Chieffi, A. Kisslinger, I. Dikic, D. Tramontano, Proline-rich tyrosine kinase 2 regulates proliferation and differentiation of prostate cells, Mol. Cell. Endocrinol. 186 (2002) 81–87.
[34] I. Ishii, N. Fukushima, X. Ye, J. Chun, Lysophospholipid receptors: signaling and biology, Annu. Rev. Biochem. 73 (2004) 321–354.
[35] M. Okita, D.C. Gaudette, G.B. Mills, B.J. Holub, Elevated levels and altered fatty acid composition of plasma lysophosphatidylcholine(lysoPC) in ovarian cancer patients, Int. J. Cancer 71 (1997) 31–34.
[36] J.J. Yan, J.S. Jung, J.E. Lee, J. Lee, S.O. Huh, H.S. Kim, K.C. Jung, J.Y. Cho, J.S. Nam, H.W. Suh, Y.H. Kim, D.K. Song, Therapeutic effects of lysophosphatidylcholine in experimental sepsis, Nat. Med. 10 (2004) 161–167.
[37] S. Takeshita, N. Inoue, D. Gao, Y. Rikitake, S. Kawashima, R. Tawa, H. Sakurai, M. Yokoyama, Lysophosphatidylcholine enhances superoxide anions production via endothelial NADH/NADPH oxidase, J. Atheroscler. Thromb. 7 (2000) 238–246.
[38] A.K. Thukkani, J. McHowat, F.F. Hsu, M.L. Brennan, S.L. Hazen, D.A. Ford, Identification of alpha-chloro fatty aldehydes and unsaturated lysophosphatidylcholine molecular species in human atherosclerotic lesions, Circulation 108 (2003) 3128–3133.
[39] B. Anliker, J. Chun, Lysophospholipid G protein-coupled receptors, J. Biol. Chem. 279 (2004) 20555–20558.
[40] I. So, M.R. Chae, S.J. Kim, S.W. Lee, Lysophosphatidylcholine, a component of atherogenic lipoproteins, induces the change of calcium mobilization via TRPC ion channels in cultured human corporal smooth muscle cells, Int. J. Impot. Res. 17 (2005) 475–483.
[41] A.J. Stokes, C. Wakano, K.A. Del Carmen, M. Koblan-Huberson, H. Turner, Formation of a physiological complex between TRPV2 and RGA protein promotes cell surface expression of TRPV2, J. Cell. Biochem. 94 (2005) 669–683.
[42] J.Y. Jung, Y.W. Kim, J.M. Kwak, J.U. Hwang, J. Young, J.I. Schroeder, I. Hwang, Y. Lee, Phosphatidylinositol 3- and 4-phosphate are required for normal stomatal movements, Plant Cell 14 (2002) 2399–2412.
[43] S.D. Sorensen, D.A. Linseman, E.L. McEwen, A.M. Heacock, S.K. Fisher, A role for a wortmannin-sensitive phosphatidylinositol-4-kinase in the endocytosis of muscarinic cholinergic receptors, Mol. Pharmacol. 53 (1998) 827–836.
[44] K. Boels, G. Glassmeier, D. Herrmann, I.B. Riedel, W. Hampe, I. Kojima, J.R. Schwarz, H.C. Schaller, The neuropeptide head activator induces activation and translocation of the growth-factor-regulated Ca(2+)-permeable channel GRC, J. Cell. Sci. 114 (2001) 3599–3606.
[45] Y. Xu, X.J. Fang, G. Casey, G.B. Mills, Lysophospholipids activate ovarian and breast cancer cells, Biochem. J. 309 (Pt. 3) (1995) 933–940.
[46] Y. Daaka, Mitogenic action of LPA in prostate, Biochim. Biophys. Acta 1582 (2002) 265–269.
[47] M.J. Caterina, T.A. Rosen, M. Tominaga, A.J. Brake, D. Julius, A capsaicin-receptor homologue with a high threshold for noxious heat, Nature 398 (1999) 436–441.
[48] J. Frederick, M.E. Buck, D.J. Matson, D.N. Cortright, Increased TRPA1, TRPM8, and TRPV2 expression in dorsal root ganglia by nerve injury, Biochem. Biophys. Res. Commun. 358 (2007) 1058–1064.
[49] C.I. Saunders, D.A. Kunde, A. Crawford, D.P. Geraghty, Expression of transient receptor potential vanilloid 1 (TRPV1) and 2 (TRPV2) in human peripheral blood, Mol. Immunol. 44 (2007) 1429–1435.